Monthly Notices
of the
ROYAL ASTRONOMICAL SOCIETY

MNRAS **428,** 212–219 (2013) doi:10.1093/mnras/sts023

Predicted properties of galactic and magellanic classical Cepheids in the SDSS filters

M. Di Criscienzo,[1]⋆ M. Marconi,[1] I. Musella,[1] M. Cignoni[2] and V. Ripepi[1]

[1]*INAF, Osservatorio Astronomico di Capodimonte, Via Moiariello 16, 80131 Napoli, Italy*
[2]*INAF, Osservatorio Astronomico di Bologna, Via Ranzani 1, 40127 Bologna, Italy*

Accepted 2012 September 17. Received 2012 September 17; in original form 2012 August 1

ABSTRACT

We present the first extensive and detailed theoretical scenario for the interpretation of Cepheid properties observed in the SDSS filters. Three sets of nonlinear convective pulsation models, corresponding to the chemical compositions of Cepheids in the Milky Way, the Large Magellanic Cloud and the Small Magellanic Cloud, respectively, are transformed into the SDSS bands by relying on updated model atmospheres. The resulting observables, namely the instability strip boundaries and the light curves, as well as the period–luminosity (PL), the Wesenheit and the period–luminosity–colour relations, are discussed as a function of the metal content, for both the fundamental and the first overtone mode. The fundamental PL relations are found to deviate from linear relations when computed over the whole observed Cepheid period range, especially at the shorter wavelengths, confirming previous findings in the Johnson–Cousins bands. The obtained slopes are found to be mildly steeper than the ones of the semi-empirical and the empirical relations available in the literature and covering roughly the same period range, with the discrepancy ranging from ∼13 per cent in u to ∼3 per cent in z.

Key words: stars: oscillations – stars: variables: Cepheids.

1 INTRODUCTION

Thanks to their characteristic period–luminosity (PL) and period–luminosity–colour (PLC) relations, classical Cepheids are the most important stellar standard candles to estimate accurate distances within the local group, reaching ∼30 Mpc from space observations. These Cepheid-based distances provide an absolute calibration of the extragalactic distance scale and two *Hubble Space Telescope* (*HST*) projects have been devoted to this issue, obtaining an estimate of the Hubble constant (see e.g. Freedman et al. 2001; Saha et al. 2001). Moreover, Cepheid properties are very important tools to investigate the physics and the evolutionary behaviour of intermediate mass stars (see e.g. Marconi 2009, and references therein). Even if the Cepheid PL and PLC relations are traditionally studied in the standard Johnson–Cousin *BVRIJK* magnitude system, the broad-band filters employed in the Sloan Digital Sky Survey (SDSS; see e.g. Abazajian et al. 2003) are becoming more and more popular in the context of current and future projects. For example, observations with the very large telescope survey telescope (VST), the Canada-France-Hawaii Telescope (CFHT), the Pan-STARRS1 survey (Kaiser 2004), the Dark Energy Survey2 (DES; Abbott et al. 2006) and the Large Synoptic Survey Telescope3 (LSST; Tyson 2002) are being done in the Sloan filters and from programmes including a time-domain component, a large number of variable stars, including Cepheids, is expected. In particular, we are deeply involved in the INAF guaranteed observing time (GTO)-approved VST survey STEP (SMC in time-evolution of a prototype interacting late-type dwarf galaxy; PI: V. Ripepi, Ripepi et al. 2006). This project will include $g_{\rm SDSS}$ and $i_{\rm SDSS}$ time series photometry of the bridge, connecting the two Magellanic Clouds, in order to study its stellar population using the variable stars as tracers. Thanks to the approved and submitted European Southern Observatory (ESO) proposal we plan to obtain 20–25 phase points in $g_{\rm SDSS}$ and $i_{\rm SDSS}$ on 32 square degrees to identify and study variables including both Classical Cepheids and RR Lyrae. Periods and mean $g_{\rm SDSS}$ and $i_{\rm SDSS}$ magnitudes will be obtained from these data and accurate PL and PLC relations will be derived.

In order to guarantee a reliable interpretation of these and other Cepheid data and to ensure a comparison between theory and observations, in this paper we provide a theoretical scenario to interpret the properties of Classical Cepheids in the SDSS filters for the characteristic chemical composition shown by these pulsators in the Milky Way and the Magellanic Clouds.

The organization of the paper is as follows. In Section 2, we present the nonlinear convective pulsation models developed by our team, whereas in Section 3 the adopted model atmospheres to transform the theoretical quantities and the bolometric light curves into the SDSS filters are discussed. The results are shown in Section 4 and in Section 5 we present the comparison between

⋆E-mail: dicrisci@gmail.com

model predictions and previous results available in the literature. The conclusions close the paper.

2 PULSATION MODELS

The adopted nonlinear convective pulsation models are taken from Bono, Marconi & Stellingwerf (1999a), Bono et al. (2001, 2002) for the chemical compositions representative of Galactic and Magellanic Cepheids, namely $Z = 0.02$, $Y = 0.28$ (Milky Way), $Z = 0.008$, $Y = 0.25$ (Large Magellanic Cloud, LMC) and $Z = 0.004$, $Y = 0.25$ (Small Magellanic Cloud, SMC). For each selected stellar mass in the range 3.5–11 $M_{\odot}$, a luminosity level is based on an evolutionary mass–luminosity relation that neglects both core overshooting and mass-loss (see Bono et al. 2001, and references therein). Previous theoretical investigation has shown that the inclusion of mild overshooting (corresponding to an increase in the intrinsic luminosity of 0.25 dex, at fixed mass, according to Chiosi, Wood & Capitanio 1993) implies a decrease of about 0.2 mag in the distance modulus inferred from theoretical Wesenheit and PLC relations (see e.g. Caputo, Marconi & Musella 2000).

The properties of adopted pulsation models are summarizedin Table 1. For each combination of chemical composition, mass and luminosity, a wide range of effective temperatures has been explored to define the position of the instability strip boundaries for both the fundamental and the first overtone (FO) mode.

Thanks to their nonlinearity these models allow us to predict the full amplitude behaviour and the variations of all the relevant quantities along a pulsation cycle. Moreover, the inclusion of a nonlocal time-dependent treatment of convection (see Stellingwerf 1982; Bono & Stellingwerf 1994; Bono et al. 1999a, for details) is the key ingredient to predict the whole topology of the instability strip,[1] as well as the detailed morphology of light, radius and radial velocity curves. The physical and numerical assumptions adopted in the computation of these models are discussed in detail in Bono, Caputo & Marconi (1998), Bono et al. (1999a), Bono, Marconi & Stellingwerf (2000a) and are not repeated here. The modal stability has been investigated in the quoted papers for both the fundamental and the FO modes, so that, moving from higher to lower effective temperatures, the following four edges are predicted for each selected chemical composition: the first overtone blue edge (FOBE), the fundamental blue edge (FBE), the first overtone red edge (FORE) and the fundamental red edge (FRE). Moreover, theoretical atlas of bolometric light curves are available (see e.g. Bono, Castellani & Marconi 2000b) for each combination of chemical composition and mass (luminosity), varying the model effective temperature (period).

3 TRANSFORMATION INTO THE SDSS PHOTOMETRIC SYSTEM

In order to obtain the pulsation observables of the investigated Cepheid models into the SDSS bands, we have transformed both the individual static luminosities and effective temperatures and the predicted bolometric light curves into the corresponding filters, using model ATLAS9 non-overshooting model atmospheres (Castelli, Gratton & Kurucz 1997a,b), convolved with the SDSS transmission functions.

[1] The existence of the red edge is related to the quenching effect of convection on pulsation.

Table 1. Parameters of the computed pulsational models adopted in this paper.The last four columns are the temperatures in Kelvin of the FOBE, FBE, FORE and FRE, respectively.

Z	$M/M_{\odot}$	$\mathrm{Log}L/L_{\odot}$	FOBE	FBE	FORE	FRE
	3.25	2.490	6650	6025	5950	5825
	3.50	2.610	6650	6025	5950	5775
	3.80	2.740	6650	6025	5950	5675
	4.00	2.820	6650	5950	5850	5625
	5.00	3.070	6450	5950	5850	5550
	5.80	3.319	6450	–	5950	–
0.004	5.50	3.400	6450	–	5950	–
	7.00	3.650	6450	–	5950	–
	7.00	3.650	6050	5950	5550	5150
	7.15	3.730	5950	5950	5650	5050
	7.30	3.760	5950	5950	5650	4950
	7.45	3.795	5950	5950	5750	4950
	9.00	4.000	–	5850	–	4850
	11.0	4.400	–	5550	–	4350
	3.25	2.450	6750	6125	6150	5875
	3.50	2.570	6650	5975	5950	5775
	3.80	2.697	6650	5950	5950	5675
	4.00	2.777	6650	5950	5850	5625
	5.00	3.070	6400	5950	5850	5450
	6.55	3.550	–	5950	–	5050
	6.70	3.586	–	5950	–	5050
0.008	6.85	3.620	–	5850	–	5050
	7.00	3.650	5850	5850	5650	4950
	7.15	3.688	–	5850	–	4950
	7.30	3.720	5850	5850	5750	4850
	7.45	3.752	–	5850	–	4850
	9.00	4.000	–	5650	–	4650
	11.0	4.400	–	5250	–	4150
	3.50	2.510	6450	–	5950	–
	4.00	2.720	6550	–	5850	–
	4.50	2.900	6350	5850	5850	5450
	5.00	3.070	6150	5950	5850	5350
	5.50	3.219	5850	–	5750	–
	5.60	3.259	5950	–	5850	–
0.02	6.25	3.420	–	5550	–	4950
	6.50	3.480	–	5650	–	4950
	6.75	3.540	–	5575	–	4850
	7.00	3.650	–	5450	–	4650
	9.00	4.000	–	5150	–	4350
	11.00	4.400	–	4850	–	3850

In particular, we used computed bolometric corrections and colour indices, as tabulated for different effective temperatures ($3500 \leq T_{\rm eff} \leq 50\,000$ K), surface gravities ($\log g$ from 0.0 to 0.5) and metallicities [$(M/H) = 0.5$, 0.2, 0.0, 0.5, 1.0, 1.5, 2.0 and 2.5, both for $(\alpha/Fe) = 0.0$ and for $(\alpha/Fe) = 0.4$], available on the homepage of Fiorella Castelli (http://www.user.oat.ts.astro.it/castelli/colors/sloan.html).

For each selected chemical composition, interpolation through these tables allowed us to obtain the static magnitudes, as well as the light curves and the resulting magnitude-averaged and intensity-averaged mean magnitudes, in the $u_{\rm SDSS}$, $g_{\rm SDSS}$, $r_{\rm SDSS}$, $i_{\rm SDSS}$ and $z_{\rm SDSS}$ filters (u, g, r, i, z in the following tables and figures).

4 PREDICTED PULSATION OBSERVABLES IN THE SDSS FILTERS

In this section, we present the results of the transformation of pulsation model predictions into the SDSS filters, providing the first

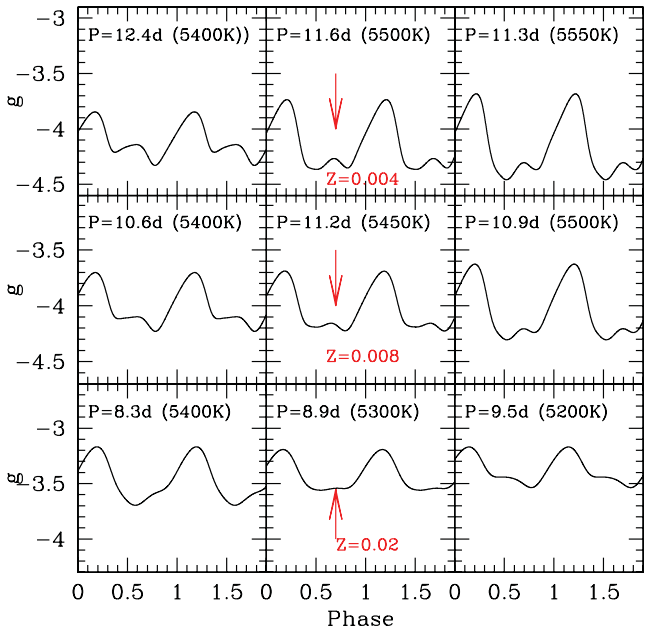

Figure 1. Theoretical atlas of light curves transformed in the g band for $Z = 0.004$ and $M = 7.15\,M_{\odot}$ (up), $Z = 0.008$ and $M = 7.15\,M_{\odot}$ (middle) and $Z = 0.02$ and $M = 6.5\,M_{\odot}$ (down). The arrow marks the position of the Hertzprung progression.

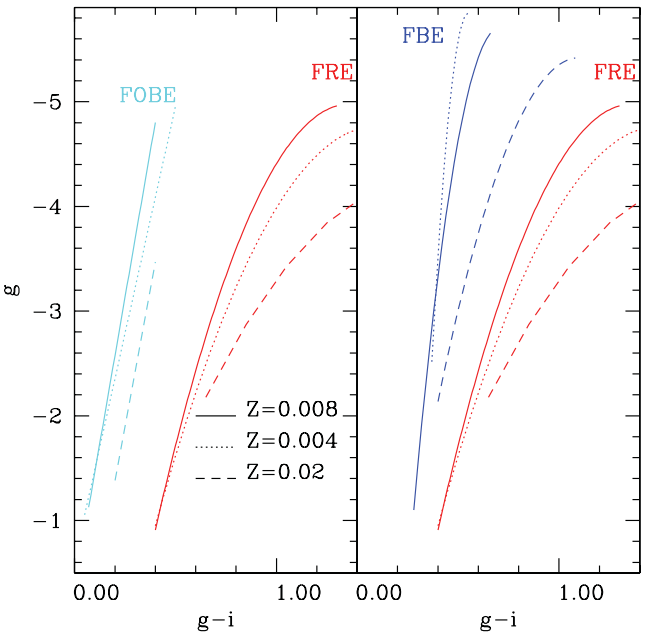

Figure 2. Predicted instability boundaries of the whole instability strip (left-hand panel) and for the fundamental mode only (right-hand panel) in the intensity-averaged g versus g–i plane for the adopted model metal abundances.

theoretical scenario to interpret observed Cepheid properties in these photometrical bands.

4.1 The light curves and the Hertzprung progression

The bolometric light curves have been transformed into the u, g, r, i and z filters. In Fig. 1, we show some examples of the resulting light curves in the g filter[2] for $Z = 0.004$ ($M = 7.15\,M_{\odot}$), $Z = 0.008$ ($M = 7.15\,M_{\odot}$) and $Z = 0.02$ ($M = 6.5\,M_{\odot}$). The behaviours shown in these plots confirm that the Hertzprung progression (Hertzsprung 1926; Ledoux & Walraven 1958), that is the relationship linking the phase of the bump and the pulsation period, occurs at $P \approx 11.5$, 11.0 and 9 d for models at $Z = 0.004$, 008 and 0.02, respectively (see e.g. Bono et al. 2000a; Marconi, Musella & Fiorentino 2005, for an extensive discussion of theoretical predictions for this phenomenon and the comparison with observations).

4.2 The instability strip boundaries

The predicted instability strip boundaries reported in the last four columns of Table 1 have been interpolated (we use a linear regression for the FOBE and FORE and a quadratic relation for the FBE and FRE) and transformed into the SDSS filters. The results are shown in Fig. 2 as a function of the adopted metallicity.

The left-hand panel of this figure shows the behaviour of the extreme edges (FOBE and FRE) of the pulsation region when moving from $Z = 0.004$ to 0.008 and $Z = 0.02$. The right-hand panel only refers to the fundamental mode (FBE and FRE).

These plots indicate that also in the g versus g–i plane, the predicted instability strip gets redder as the metallicity increases. In particular, the nonlinear trend and the metallicity effect, shown in the right-hand panel for the fundamental mode boundaries, are known to directly reflect into the behaviour of the predicted fundamental PL relations (see Bono et al. 1999b). In other words, on the basis of the behaviours noted in this figure, the PL relation in the g filter is expected to be nonlinear and metallicity dependent.

4.3 Colour–colour relations

The transformed multifilter light curves can be reported in different colour–colour planes. In Fig. 3, we show the theoretical fundamental (F) and FO pulsators in the r–i versus g–r, i–z versus r–i and g–r versus g–i diagrams for the adopted metallicities.

On the contrary of what happened in the g–r versus u–g plane, due to the significant sensitivity of the u band on metal abundance, in the colour–colour plane reported in the figures, the relations are very narrow and the effect of metallicity is smaller. In particular, this effect becomes negligible for the g–i and g–r combination of colours suggesting that the comparison between theory and observations in this plane could be used to evaluate colour excesses.

The linear regression through the intensity-averaged mean magnitudes of synthetic F and FO pulsators (see subsection 4.4) provides the following metal-dependent analytical colour–colour relations:

$$g-r = 0.12 + 2.34(r-i) \quad (\sigma = 0.009)$$

$$i-z = -0.04 + 0.62(r-i) \quad (\sigma = 0.002)$$

$$g-r = 0.04 + 0.70(g-i) \quad (\sigma = 0.003)$$

for $Z = 0.004$.

$$g-r = 0.12 + 2.35(r-i) \quad (\sigma = 0.008)$$

$$i-z = -0.04 + 0.63(r-i) \quad (\sigma = 0.002)$$

$$g-r = 0.04 + 0.70(g-i) \quad (\sigma = 0.002)$$

[2] The light curves in the other filters and for other stellar masses are available upon request to the authors.

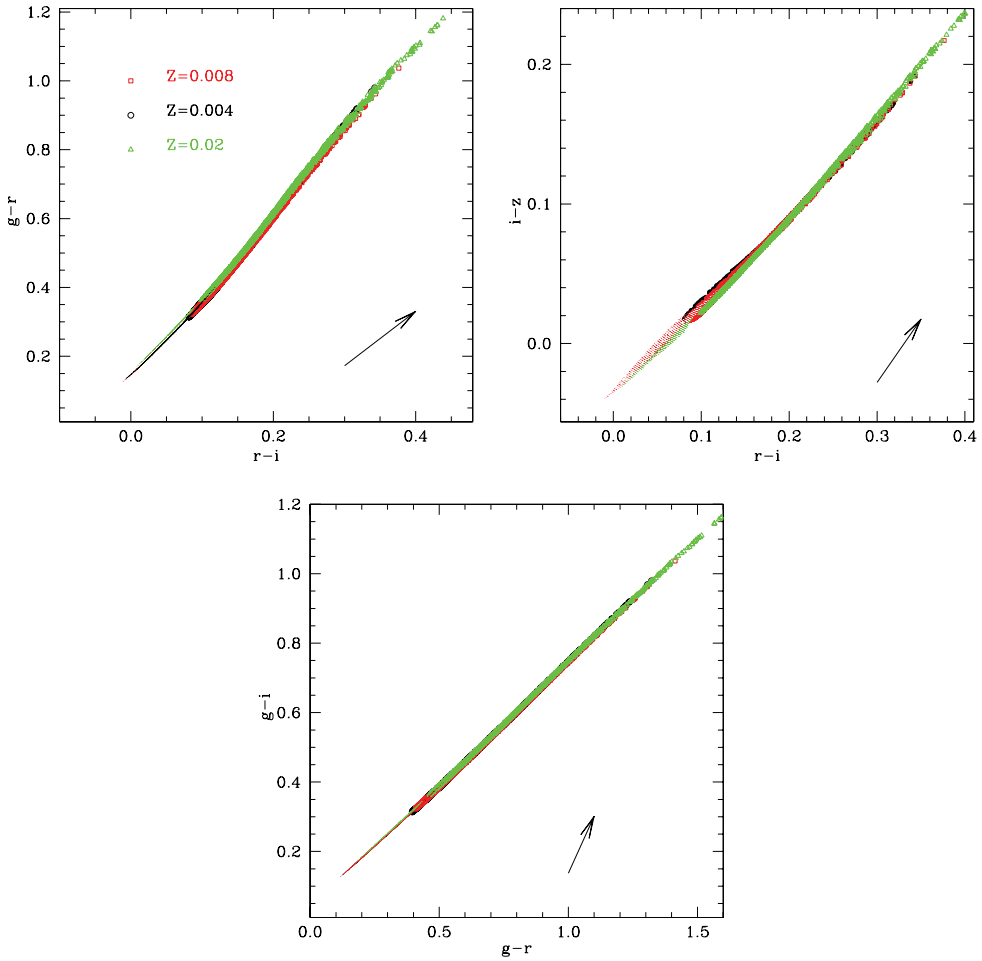

Figure 3. Fundamental and FO (smaller points on the left-hand side of each figure) models of different metallicities in colour–colour planes. A reddening vector for $A_V = 0.5$ is also shown in each panel.

for $Z = 0.008$.

$$g-r = 0.12 + 2.44(r-i) \quad (\sigma = 0.008)$$

$$i-z = -0.04 + 0.67(r-i) \quad (\sigma = 0.003)$$

$$g-r = 0.04 + 0.71(g-i) \quad (\sigma = 0.002)$$

for $Z = 0.02$.

4.4 Period–luminosity relations

We used the synthetic distributions of fundamental models computed by Caputo, Marconi & Musella (2000) to derive the PL relations for different photometric bands listed in Table 2 for the three assumed chemical compositions. We fitted with a linear regression M_i = a+b Log$P$ the predicted distribution of F pulsators for different assumptions on the period range, namely log $P \leq 2.0$, log $P \leq 1.5$, log $P \leq 1.0$ and log $P \geq 1.0$ to determine the three corresponding slopes: $b_{\rm all}$, $b_{\leq 1.5}$, $b_{\rm short}$ and $b_{\rm long}$. The investigation of the difference between $b_{\rm short}$ and $b_{\rm long}$ is relevant in the context of current studies in the literature claiming the existence of a break at 10 d (see e.g. Caputo et al. 2000; Sandage, Tammann & Reindl 2004; Marconi et al. 2005; Ngeow, Kanbur & Nanthakumar 2008). As shown in Fig. 4, the PL relations get steeper by increasing the filter wavelength, in agreement with the well-known empirical and theoretical results in Johnson–Cousins photometric bands (Madore & Freedman 1991; Caputo et al. 2000), as well as with the semi-empirical PL relations in the Sloan bands derived by Ngeow & Kanbur (2007).

Moreover, in agreement with the results by Bono (2010), the slopes of the relations at Log $P \leq 1.0$ are steeper than those for longer periods, indicating a clear break of the PL relation at 10 d, more evident for the Magellanic Cloud chemical compositions, in agreement with empirical suggestions. However, the amplitude of this effect decreases as the filter wavelength increases. In the case of FO pulsators that are intrinsically limited to a shorter period range, linear relations over the whole covered period range are derived.

The results reported in Table 2 clearly show the expected flattening of the various fundamental PL relations when the metallicity increases. Again, this trend decreases as the wavelength increases.

The smaller, negligible passing from $Z = 0.004$ to 0.008, sensitivity to metallicity of FO PL relations is due to the much narrower instability strip that is also hotter than the one of fundamental pulsators, and in turn less affected by changes in the convective efficiency produced by metallicity variations.

Table 2. Predicted slopes of fundamental and FO PL relations in the SDSS filters. Columns from second to fourth report the slopes in three different assumptions on the period range, namely $\log P \leq 2.0$, $\log P \leq 1.0$ and $\log P \geq 1.0$ and $\log P \leq 1.5$. The last column reports the slopes of FO PL relations over the whole period range covered by models.

Band	$b_{\rm F,all}$	$b_{\rm F,short}$	$b_{\rm F,long}$	$b_{\rm F,\leq 1.5}$	$b_{\rm FO,all}$
$Z = 0.004$					
u	−2.503(0.016)	−3.134(0.016)	−0.897(0.088)	−2.752(0.014)	−2.963(0.015)
g	−2.893(0.012)	−3.362(0.015)	−1.789(0.066)	−3.065(0.012)	−3.136(0.016)
r	−3.098(0.009)	−3.440(0.011)	−2.301(0.050)	−3.222(0.009)	−3.291(0.012)
i	−3.177(0.008)	−3.469(0.010)	−2.494(0.043)	−3.281(0.008)	−3.363(0.010)
z	−3.231(0.007)	−3.494(0.009)	−2.620(0.038)	−3.326(0.007)	−3.410(0.009)
$Z = 0.008$					
u	−2.274(0.016)	−2.875(0.016)	−0.849(0.088)	−2.498(0.015)	−2.751(0.013)
g	−2.707(0.012)	−3.131(0.014)	−1.766(0.065)	−2.855(0.012)	−2.919(0.014)
r	−2.949(0.099)	−3.257(0.011)	−2.265(0.049)	−3.056(0.009)	−3.080(0.010)
i	−3.044(0.008)	−3.309(0.009)	−2.459(0.042)	−3.137(0.008)	−3.155(0.008)
z	−3.109(0.007)	−3.346(0.009)	−2.588(0.038)	−3.192(0.007)	−3.206(0.007)
$Z = 0.02$					
u	−1.156(0.0232)	−1.833(0.038)	−0.361(0.070)	−1.503(0.025)	−2.908(0.024)
g	−1.973(0.015)	−2.307(0.031)	−1.558(0.047)	−2.151(0.018)	−3.101(0.024)
r	−2.396(0.011)	−2.632(0.023)	−2.092(0.035)	−2.527(0.013)	−3.299(0.018)
i	−2.562(0.10)	−2.763(0.020)	−2.306(0.030)	−2.672(0.010)	−3.390(0.016)
z	−2.680(0.009)	−2.852(0.017)	−2.460(0.027)	−2.774(0.007)	−3.449(0.014)

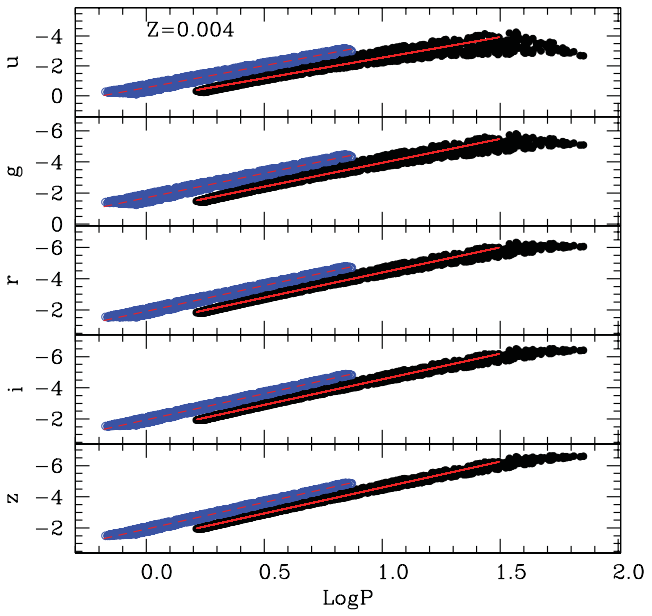

Figure 4. PL relations ($\log P \leq 1.5$, see Table 2) in different SDSS photometrical bands for fundamental (solid lines) and FO (dashed lines) models with $Z = 0.004$. The same figures for $Z = 0.008$ and $Z = 0.02$ are given in the online version of the paper.

Table 3. The Wesenheit relations for fundamental and FO pulsators with different metallicities.

$W = a + b \log P$				
W		a	b	rms
$Z = 0.004$				
g-4.099(g–r)	F	−2.01	−3.73	0.02
	FO	−2.58	−3.77	0.01
g-2.354(g–i)	F	−1.79	−3.56	0.03
	FO	−2.28	−3.67	0.03
g-1.722(g–z)	F	−1.58	−3.48	0.06
	FO	−2.10	−3.61	0.04
$Z = 0.008$				
g-4.099(g–r)	F	−2.11	−3.70	0.02
	FO	−2.55	−3.58	0.01
g-2.354(g–i)	F	−1.79	−3.50	0.04
	FO	−2.25	−3.47	0.01
g-1.722(g–z)	F	−1.58	−3.40	0.06
	FO	−2.07	−3.41	0.03
$Z = 0.02$				
g-4.099(g–r)	F	−2.131	−3.71	0.015
	FO	−2.641	−3.91	0.007
g-2.354(g–i)	F	−1.89	−3.36	0.03
	FO	−2.32	−3.78	0.02
g-1.722(g–z)	F	−1.70	−3.19	0.05
	FO	−2.11	−3.70	0.03

4.5 The Wesenheit relations

As the PL relation reflects the instrinsic width of the instability strip and its application implies the availability of a statistically significant sample, as well as the need to disentangle reddening and metallicity effects on distance determinations (see discussions in Caputo, Marconi & Ripepi 1999; Caputo et al. 2000, 2001), the reddening free Wesenheit relation is often preferred. The latter relies on an assumed reddening law and includes a colour term similar, but not identical, to the PLC colour term (see below), thus partially reducing the effect of the finite width of the instability strip (see Caputo et al. 2000). The predicted Wesenheit functions in the SDSS filters have been built by adopting the colour coefficients given by Giradi et al. (2004) and are reported inTable 3 for both the fundamental and the FO mode. These results clearly indicate the decrease in the intrinsic dispersion when passing from the PL to the Wesenheit relations, in agreement with previous empirical and theoretical results (Madore & Freedman 1991; Caputo et al. 2000; Ripepi et al. 2012). The obtained Wesenheit relations for $Z =$ 0.004 are shown in Fig. 5. These plots confirm the linearity and the

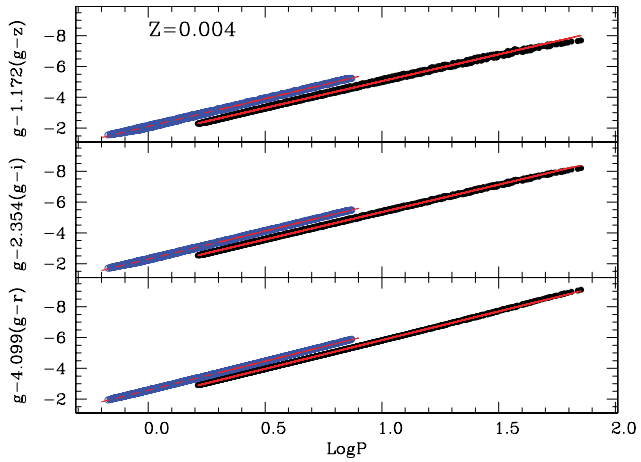

Figure 5. Wesenheit relations in different SDSS photometrical bands for fundamental (solid line) and FO (dashed line) models with $Z = 0.004$ The same figures for $Z = 0.008$ and $Z = 0.02$ are given in the on-line version of the paper.

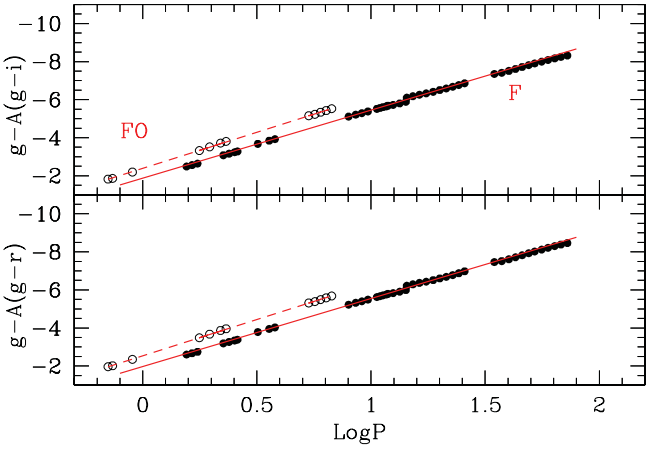

Figure 6. PLC relations for F (closed circles) and FO (open circles) models with $Z = 0.004$. See also Table 4.

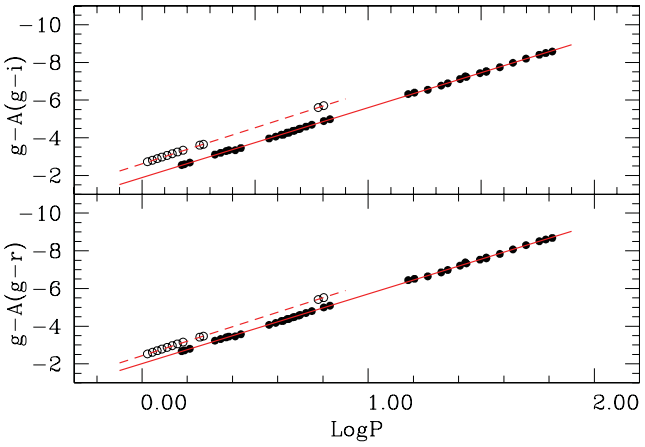

Figure 7. As for Fig. 6 but for $Z = 0.004$.

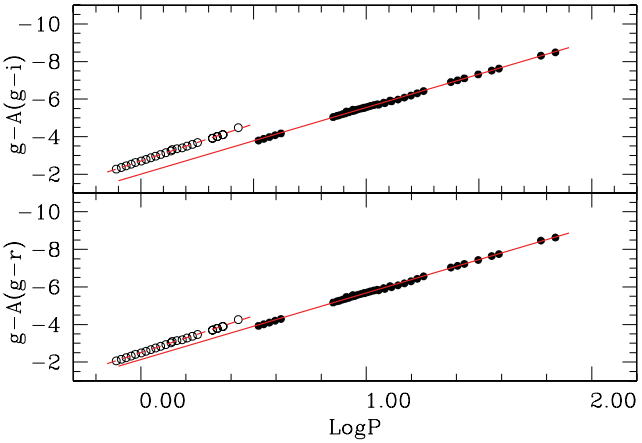

Figure 8. As for Fig. 6 but for $Z = 0.02$.

small intrinsic dispersion of the Wesenheit relations that make them powerful tools to infer Galactic and extragalactic Cepheid distances.

We note that in agreement with previous results in the Johnson–Cousins bands (Caputo et al. 2000), the metallicity dependence of the Wesenheit relations is reversed when passing from optical to near-infrared colours with the smallest effect for the g, $g-r$ combination.

4.6 The PLC relations

The Wesenheit relations are reddening free but only partially correcting the effect of the finite width of the instability strip with the inclusion of their colour term. However, the true relation that holds for each individual Cepheid is the PLC relation, directly descending from the combination of the period–density, the Stephan–Boltzmann and the evolutionary mass–luminosity relations (see e.g. Bono et al. 1999b; Marconi 2009, and references therein). The disadvantage is that both individual reddening and multiband photometry are required in order to apply PLC relations to infer Cepheid distances and this is the reason why these relations are rarely adopted in the literature. In any case, the theoretical SDSS PLC relations based on the adopted pulsation and atmosphere models are reported in Table 4 and shown in Figs 6, 7 and 8. We note that differently

Table 4. PLC relations for fundamental and FO pulsators with different metallicities.

$g = a$ colour $+b \log P+c$	colour	a	b	c	rms
$Z = 0.004$					
F	$(g–r)$	3.99	−3.65	−2.06	0.04
	$(g–i)$	2.87	−3.66	1.96	0.04
FO	$(g–r)$	4.01	−3.80	−2.54	0.02
	$(g–i)$	2.79	−3.79	−2.39	0.02
$Z = 0.008$					
F	$(g–r)$	3.99	−3.70	−2.01	0.03
	$(g–i)$	2.85	−3.71	−1.89	0.03
FO	$(g–r)$	4.32	−3.83	−2.62	0.01
	$(g–i)$	2.96	−3.83	−2.44	0.01
$Z = 0.02$					
F	$(g–r)$	3.86	−3.55	−2.13	0.05
	$(g–i)$	2.75	−3.55	−2.00	0.04
FO	$(g–r)$	4.32	−3.93	−2.71	0.03
	$(g–i)$	2.93	−3.92	−2.50	0.03

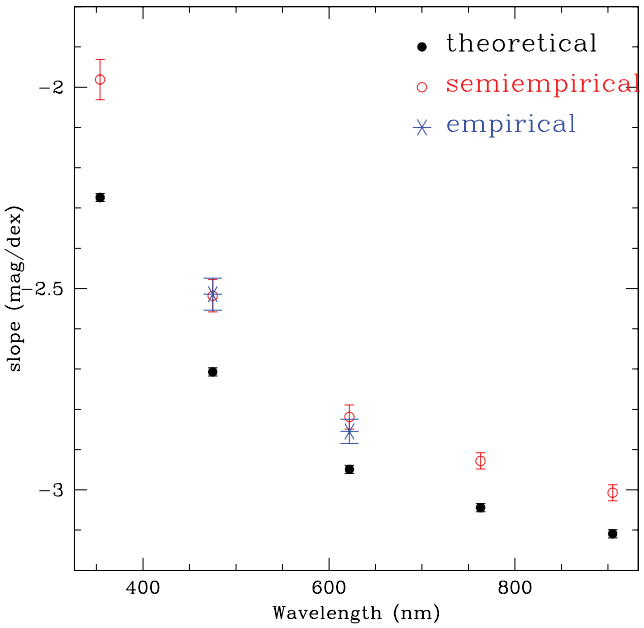

Figure 9. Comparison between the slopes of the theoretical PL relations derived in this paper and the semi-empirical and empirical ones by Ngeow & Kanbur (2007).

from the PL and the Wesenheit relations, the PLC ones have been derived from the individual pulsating models and not from the simulated Cepheid distributions within the respective instability strips. This, because of the mentioned intrinsic nature of these relations, is expected to hold for each individual pulsator. Again we find a smaller metallicity effect in the case of FO models.

5 COMPARISON WITH PREVIOUS RELATIONS IN THE LITERATURE

In a recent paper, Ngeow & Kanbur (2007) have derived semi-empirical Cepheid PL relations in the SDSS magnitudes by combining observed LMC BVI mean magnitudes with theoretical bolometric corrections. In the same paper, these authors construct empirical g, r PL relations, using the publicly available Johnson–Sloan photometric transformations, finding a good agreement with the semi-empirical ones.

In Fig. 9, we show the comparison between the PL slopes derived in this paper for fundamental models with $Z = 0.008$ and $\log P < 2.0$ (filled symbols) and the semi-empirical ones (Ngeow & Kanbur 2007, open symbols) for the u, g, r, i, z filters. In the case of g and r, the empirical relations by the same authors (asterisks) are also shown. These comparisons suggest that the slope of the PL relations obtained in this paper, using suitable pulsation and atmosphere models, for periods shorter than 100 d, is systematically steeper than the semi-empirical and empirical ones presented by Ngeow & Kanbur (2007), with a deviation decreasing from ∼13 per cent in the u filter to ∼3 per cent in the z filter.

6 CONCLUSIONS

In this paper, we have provided the first theoretical scenario to our knowledge for the interpretation of classical Cepheid properties observed in the SDSS filters. Extensive and detailed sets of nonlinear convective pulsation models computed for the typical chemical compositions of Galactic and Magellanic pulsators have been transformed into the SDSS filters by using bolometric corrections and colour–temperature transformations based on updated model atmospheres. The main results of this investigation can be summarized as follows.

(i) The transformed instability strip confirms the nonlinearity of the fundamental boundaries and the dependence on the metal content already found in the Johnson–Cousins bands. This behaviour explains why PL relations are not linear at large periods.

(ii) The PL relations in the SDSS filters show evidence of the break at 10 d, in particular for the lower metal contents and the shorter wavelengths, as expected on the basis of previous empirical and theoretical studies.

(iii) The theoretical light curves in the SDSS filters present morphological characteristics similar to the ones in the Johnson–Cousins bands, with evidence of the Hertzprung-progression phenomenon at the expected period for each selected chemical composition.

(iv) The derived Wesenheit and PLC relations have, as expected, a smaller intrinsic dispersion than PL relations and show a metallicity dependence that resembles the behaviour of their Johnson–Cousins counterparts.

(v) The obtained relations for FO pulsators are all linear and much less affected by metallicity than the fundamental mode ones.

(vi) A comparison between the relations obtained in this paper and the semi-empirical and empirical ones obtained by Ngeow & Kanbur (2007) indicates a discrepancy in the slopes ranging from ∼13 per cent in u to ∼3 per cent in z, with the theoretical relations being systematically steeper.

ACKNOWLEDGMENTS

We want to thank the anonymous reviewer for the constructive comments. Financial support for this research was provided by PRIN INAF 2011 ‘Tracing the formation and evolution of the Galactic halo with VST’ P.I. Marconi. In particular MDC acknowledges the support of INAF through the 2011 postdoctoral fellowship grant.

REFERENCES

Abazajian K. et al., 2003, AJ, 126, 2081
Abbott T. M. C. et al., 2006, Proc. SPIE, 6267E.119A
Bono G., 2010, Mem. Soc. Astron. Ital., 81, 863
Bono G., Stellingwerf R. F., 1994, ApJS, 93, 233
Bono G., Caputo F., Marconi M., 1998, ApJ, 497, L43
Bono G., Marconi M., Stellingwerf R. F., 1999a, ApJS, 122, 167
Bono G., Caputo F., Castellani V., Marconi M., 1999b, ApJ, 512, 711
Bono G., Marconi M., Stellingwerf R. F., 2000a, A&A, 360, 245
Bono G., Castellani V., Marconi M., 2000b, ApJ, 529, 293
Bono G., Gieren W. P., Marconi M., Fouqué P., Caputo F., 2001, ApJ, 563, 319
Bono G., Groenewegen M. A. T., Marconi M., Caputo F., 2002, ApJ, 574, L33
Caputo F., Marconi M., Ripepi V., 1999, ApJ, 525, 784
Caputo F., Marconi M., Musella I., Santolamazza P., 2000, A&A, 359, 1059
Caputo F., Marconi M., Musella I., 2000, A&A, 354, 610
Caputo F., Marconi M., Musella I., Pont F., 2001, A&A, 372, 544
Castelli F., Gratton R. G., Kurucz R. L., 1997a, A&A, 318, 841
Castelli F., Gratton R. G., Kurucz R. L., 1997b, A&A, 324, 432
Chiosi C., Wood P. R., Capitanio N., 1993, ApJS, 86, 541C
Freedman W. L. et al., 2001, ApJ, 553, 47
Girardi L., Grebel E. K., Odenkirchen M., Chiosi C., 2004, A&A, 422, 205G
Hertzsprung E., 1926, Bull. Astron. Inst. Netherlands, 3, 115
Kaiser N., 2004, Proc. SPIE, 5489, 11K

Ledoux P., Walraven T., 1958, in Flügge S., ed., Handbuch der Physik. Springer, New York, p. 353
Madore B. F., Freedman W. L., 1991, PASP, 103, 933
Marconi M., 2009, MnSAI, 80, 141
Marconi M., Musella I., Fiorentino G., 2005, ApJ, 632, 590
Ngeow C., Kanbur S. M., 2007, ApJ, 667, 35
Ngeow C., Kanbur S. M., Nanthakumar A., 2008, A&A, 477, 621
Ripepi V. et al., 2006, MSAIS, 9, 267
Ripepi V. et al., 2012, MNRAS, 424, 1807
Saha A. et al., 2001, ApJ, 562, 314
Sandage A., Tammann G. A., Reindl B., 2004, A&A, 424, 43
Stellingwerf R. F., 1982, ApJ, 262, 330
Tyson J. A., 2002, Proc. SPIE, 4836, 10T

This paper has been typeset from a TEX/LATEX file prepared by the author.